



## Tunable surface conductivity in Bi<sub>2</sub>Se<sub>3</sub> revealed in diffusive electron transport

J. Chen,<sup>1</sup> X. Y. He,<sup>1</sup> K. H. Wu,<sup>1</sup> Z. Q. Ji,<sup>1</sup> L. Lu,<sup>1</sup> J. R. Shi,<sup>2</sup> J. H. Smet,<sup>3</sup> and Y. Q. Li<sup>1</sup>

<sup>1</sup>*Institute of Physics, Chinese Academy of Sciences, and Beijing National Laboratory for Condensed Matter Physics, Beijing 100190, China*

<sup>2</sup>*International Center for Quantum Materials, Peking University, Beijing 100871, China*

<sup>3</sup>*Max Planck Institute for Solid State Research, D-70569, Stuttgart, Germany*

(Received 23 March 2011; revised manuscript received 27 April 2011; published 14 June 2011)

We demonstrate that the weak antilocalization effect can serve as a convenient method for detecting decoupled surface transport in topological insulator thin films. In the regime where a bulk Fermi surface coexists with the surface states, the low-field magnetoconductivity is well described by the Hikami-Larkin-Nagaoka equation for single-component transport of noninteracting electrons. When the electron density is lowered, the magnetotransport behavior deviates from the single-component description and strong evidence is found for independent conducting channels at or near the bottom and top surfaces. The magnetic-field-dependent part of corrections to conductivity due to Zeeman energy is shown to be negligible for the fields relevant to the weak antilocalization despite considerable electron-electron interaction effects on the temperature dependence of the conductivity.

DOI: [10.1103/PhysRevB.83.241304](https://doi.org/10.1103/PhysRevB.83.241304)

PACS number(s): 73.25.+i, 03.65.Vf, 71.70.Ej, 72.15.Rn

The surface of a three-dimensional (3D) topological insulator (TI)<sup>1,2</sup> hosts a two dimensional (2D) system of Dirac electrons with spins transversely locked to their translational momenta. Such spin-helical surface states<sup>3</sup> offer a new route for realizing exotic entities such as Majorana fermions and magnetic monopoles.<sup>4</sup> The unique surface spin structure also has a profound impact on the transport properties of TIs.<sup>1,5</sup> The Berry phase associated with the surface electrons causes suppression of backscattering<sup>6</sup> and hence immunity to localization regardless of the strength of disorder.<sup>5</sup> This weak antilocalization effect can be brought out by applying a perpendicular magnetic field. It produces a negative magnetoconductivity due to the breaking of time-reversal symmetry. The negative magnetoconductivity has indeed been observed in various TI thin films by several groups.<sup>7-11</sup> However, most of these measurements were carried out with samples in which the Fermi energy is not located in the band gap, so that they are not in the so-called topological transport regime.<sup>12,13</sup> Since topologically trivial 2D electron systems (e.g., Au thin films) may also exhibit similar magnetoconductivity behavior as long as the spin-orbit coupling (SOC) is sufficiently strong,<sup>14</sup> concern has to be raised about whether weak antilocalization can provide a reliable method for identifying the surface-state transport, which is a key starting point for future exploration of various topological effects and novel devices.<sup>1,15-18</sup>

Here we confirm unequivocally that the weak antilocalization effect can be used to differentiate the surface transport from that dominated by bulk carriers. This is demonstrated on Bi<sub>2</sub>Se<sub>3</sub> thin films with carrier densities that can be tuned over a wide range with a back gate. When the transport is not in the topological regime, the magnetoconductivity can be described by a single-component Hikami-Larkin-Nagaoka (HLN) equation.<sup>19</sup> This description is found to be valid for a remarkably wide range of electron densities (0.8–8.6 × 10<sup>13</sup> cm<sup>-2</sup>) in samples with the Fermi energy located inside the conduction band, even if electron-electron interactions are taken into account. In contrast, in a regime where the electronic system is split up into an electron layer at the top surface and a hole layer at the bottom, the magnetoconductivity deviates strongly from the single-component HLN equation. Our

analysis provides a convenient method for detecting decoupled surface transport. It complements existing techniques based on quantum oscillations that are limited to samples of high carrier mobilities<sup>20</sup> or samples with a quasi-one-dimensional (1D) geometry.<sup>21</sup>

The Bi<sub>2</sub>Se<sub>3</sub> thin films were grown on SrTiO<sub>3</sub>(111) substrates with molecular beam epitaxy.<sup>22</sup> The dielectric properties of SrTiO<sub>3</sub> are well suited for gating purposes and the carrier density in these devices can be varied by at least 2 × 10<sup>13</sup> cm<sup>-2</sup>.<sup>7</sup> All of the samples used in this work were patterned into 50-μm-wide Hall bars with photolithography, followed by Ar plasma etching (Fig. 1, inset). This eliminates uncertainties in evaluating resistivities encountered in previous transport studies due to the influence of electrical contacts or the irregular shape of the sample. A set of more than ten samples with thicknesses between 5 and 20 nm has been measured. Most of the samples have a back gate deposited at the bottom of the substrate, and a few of them are additionally equipped with a top gate. The latter was deposited on an AlO<sub>x</sub> layer prepared with atomic layer deposition. Transport measurements were carried out in cryostats with temperatures as low as 10 mK and magnetic fields up to 18 T.

Figure 1 displays typical magnetotransport data. All of the samples show a positive magnetoresistance with a sharp cusp around zero magnetic field, consistent with previous measurements of Bi<sub>2</sub>Se<sub>3</sub> thin films.<sup>7-11</sup> As demonstrated in Fig. 1(b), the low-field magnetoconductivity, defined as  $\Delta\sigma(B) = \sigma_{xx}(B) - \sigma_{xx}(0)$ , can be fitted well with the HLN equation in the strong SOC limit, i.e., when  $\tau_\phi \gg \tau_{so}, \tau_e$ :

$$\Delta\sigma(B) \simeq -\alpha \frac{e^2}{\pi h} \left[ \psi \left( \frac{1}{2} + \frac{B_\phi}{B} \right) - \ln \left( \frac{B_\phi}{B} \right) \right], \quad (1)$$

where  $\tau_{so}$  ( $\tau_e$ ) is the spin-orbit (elastic) scattering time,  $\psi$  is the digamma function,  $B_\phi = \hbar/(4De\tau_\phi)$  is a characteristic field related to the dephasing time  $\tau_\phi$ ,  $D$  is the diffusion constant, and  $h$  is the Planck constant. The coefficient  $\alpha$  takes a value of 1/2 for a traditional 2D electron system with strong spin-orbit coupling. The same value is expected for the electron transport on one surface of a 3D TI with a single Dirac cone.<sup>7</sup>

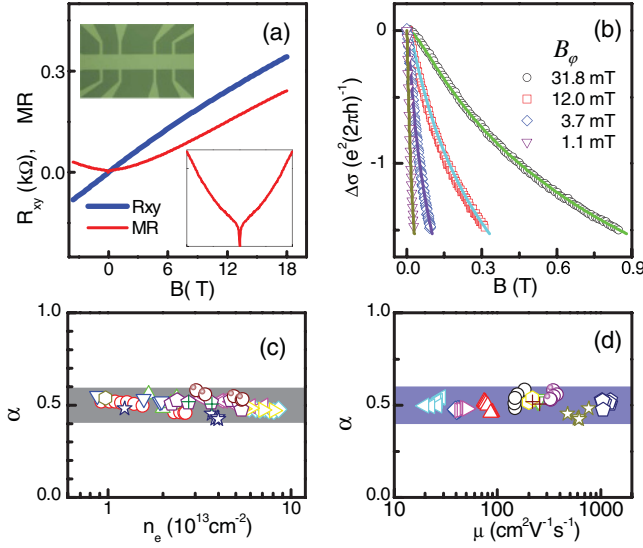


FIG. 1. (Color online) (a) Magnetoresistance [MR, defined as  $\rho_{xx}(B)/\rho_{xx}(0) - 1$ ] and Hall resistance of a typical  $\text{Bi}_2\text{Se}_3$  thin film at  $T = 1.2$  K. The low-field MR (between  $\pm 3$  T) is shown more clearly in the lower inset. The upper inset is an optical image of the Hall bar used for the transport measurements. (b) Magnetoconductivity data (symbols) from four samples fitted with Eq. (1) (lines). The dephasing field  $B_\phi$  varies by nearly a factor of 30. Extracted values of  $\alpha$  for ten samples are plotted as a function of electron density  $n_e$  and mobility  $\mu$  in (c) and (d), respectively. They are evaluated with  $n_e = 1/(eR_H)$  and  $\mu = R_H/\rho_{xx}(0)$  at low fields.

Figure 1(c) shows that the extracted  $\alpha$  values are distributed in a narrow range near  $1/2$  for ten samples with 2D electron densities  $n_e$  spreading from  $0.8$  to  $8.6 \times 10^{13} \text{ cm}^{-2}$ .<sup>23</sup> No correlation is found between  $\alpha$  and the electron mobility  $\mu$ , which varies nearly two orders of magnitude [Fig. 1(d)]. Based on angle-resolved photoemission measurements,<sup>12</sup> the top and bottom surfaces of a  $\text{Bi}_2\text{Se}_3$  thin film can only accommodate a total electron density of  $\sim 0.5 \times 10^{13} \text{ cm}^{-2}$  even if the Fermi energy reaches the bottom of the conduction band. Thus we anticipate a significant number of bulk electrons (or quasi-2D electrons with parabolic dispersion) for the above range of  $n_e$ . The nonlinear Hall resistivity curves [see e.g., Fig. 1(a)] also suggest the coexistence of multiple charge-carrier types. Even if so, the analysis of the weak antilocalization effect itself at small magnetic fields yields values of  $\alpha$  close to  $1/2$ . In this magnetic field regime where the antilocalization effect is observed, these samples behave like 2D systems with a single type of charge carrier. This can only be understood when there is a strong mixing between the surface and the bulk electron states or when the dephasing field of one of the conducting components (i.e., the bulk or top/bottom surface) is much smaller than those of the others. We note that it was demonstrated long ago that the two-valley 2D electron system confined in a Si inversion layer displays  $\alpha$  values close to that for a single-valley system and not the one expected for two independent valleys.<sup>24</sup> Fukuyama attributed it to intervalley scattering.<sup>25</sup> Similar physics might take place here because of considerable scattering between the surface and bulk states when the Fermi energy is located in the conduction band.

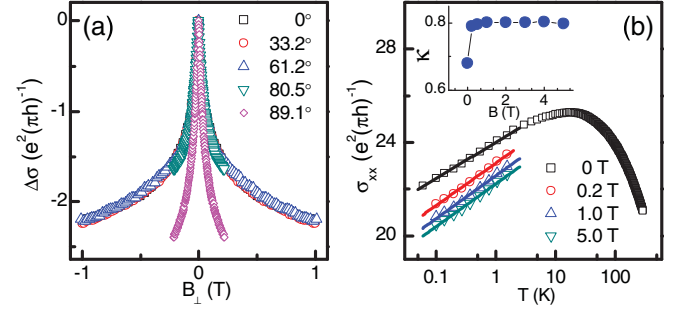


FIG. 2. (Color online) (a) Magnetoconductivity  $\Delta\sigma(B)$  at  $T = 2$  K and  $V_G = 0$  V plotted as a function of perpendicular magnetic field  $B_\perp$  for several tilt angles.  $\theta = 0$  refers to  $\mathbf{B}$  perpendicular to the thin-film plane. (b) Temperature dependencies of  $\sigma_{xx}$  (open symbols) recorded at  $B = 0, 0.2, 1,$  and  $5$  T. The straight lines are linear fits of  $\sigma_{xx}$  to  $\ln T$ . In the upper inset, the slope, defined as  $\kappa = (\pi h/e^2)d\sigma_{xx}(B, T)/d(\ln T)$ , is plotted as a function  $B$ . The electron density is about  $2 \times 10^{13} \text{ cm}^{-2}$  so that  $E_F$  is located in the conduction band.

The robustness of  $\alpha \simeq 1/2$  is at first sight surprising, because sources other than weak antilocalization may also contribute to the low-field magnetoconductivity. In the non-interacting electron picture, the Zeeman energy, which was not considered in deriving the HLN equation, is known for mixing the spin singlet and triplet states and hence suppressing the weak antilocalization effect.<sup>26</sup> The corresponding correction to  $\Delta\sigma(B)$  is determined by the ratio  $\gamma = E_Z/E_{so} = g\mu_B B/(\hbar\tau_{so}^{-1})$ , where  $g$  is the electron  $g$  factor. The Zeeman energy also causes an extra change in  $\Delta\sigma(B)$  if electron-electron interactions are not negligible in the diffusion channel.<sup>27,28</sup> The corresponding correction to the conductivity is  $\Delta\sigma_I(B) = \frac{e^2}{\pi h} \frac{\tilde{F}^\sigma}{2} g_2(\tilde{h})$  with  $\tilde{h} = E_Z/k_B T$ , where  $\tilde{F}^\sigma$  is a parameter reflecting the strength of the dynamically screened Coulomb interaction.

Since the electron  $g$  factor of bulk  $\text{Bi}_2\text{Se}_3$  is quite large,<sup>29</sup> one would expect sizable Zeeman corrections to  $\Delta\sigma(B)$ . This appears to be in contradiction with the data recorded in tilted magnetic fields and plotted in Fig. 2(a). The low-field magnetoconductivity exhibits very little angular dependence for tilt angles less than  $80^\circ$ . Considering that  $E_Z$  nearly doubles (triples) for  $\theta = 60^\circ$  ( $70^\circ$ ) with respect to the zero-tilt case, we conclude that the influence of the Zeeman energy can be neglected in the case of zero or small tilts. In the noninteracting regime, this can be understood as a consequence of strong SOC, and hence small  $\gamma$  for the fields of interest. Also, in the regime where  $e$ - $e$  interactions are important, the strong SOC suppresses the Zeeman contribution. The Zeeman term was derived under the assumption of weak SOC.<sup>27</sup> Theories<sup>27,28,30</sup> and experiments<sup>31</sup> on other materials have clearly shown that strong SOC can diminish and even entirely suppress the Zeeman-split term in the diffusion channel.

The effects of strong SOC are further manifested in the temperature dependence of  $\sigma_{xx}$  displayed in Fig. 2(b). The slope of the  $\Delta\sigma(B)$ - $\ln T$  plot, defined as  $\kappa = (\pi h/e^2)d\sigma_{xx}(B, T)/d(\ln T)$ , is nearly constant for  $B = 0.2$ – $5$  T. Both weak antilocalization and  $e$ - $e$  interactions can cause the  $\ln T$  dependence.<sup>14,27</sup> The weak antilocalization effect, however, only produces a pronounced  $T$  dependence to  $\sigma_{xx}$

at zero or low magnetic fields. The nearly constant slope at  $B > 0.2$  T can be attributed to the strong SOC, which suppresses the triplet terms.<sup>5,30</sup> They would otherwise produce  $\ln T$  corrections proportional to  $\tilde{F}^\sigma$ .<sup>27,30</sup> Hence,  $\kappa = 1$  is expected<sup>5</sup> for sufficiently large  $B$ . The observed  $\kappa \simeq 0.8$  is slightly smaller. This deviation may originate from other sources such as the corrections in the Cooperon channel.<sup>32</sup> Nevertheless, the nearly constant  $\kappa$  for  $B = 0.2$ –5 T indicates that the  $e$ - $e$  interactions do not induce significant corrections to  $\Delta\sigma(B)$  in lower fields, where the weak antilocalization is pronounced. As to the zero-field conductivity, the combined effects of  $e$ - $e$  interactions and weak antilocalization lead to a  $\ln T$  dependence with  $\kappa = 1 - 1/2 = 1/2$ , which is qualitatively in agreement with our data and others.<sup>10,11</sup> Taking this together with the tilted-field data, we can conclude that the single-particle HLN equation in the strong SOC limit [Eq. (1)] can provide a good description of the low-field magnetoconductivity for a conducting 2D channel with strong SOC or one surface of a 3D TI.

Now we are in a position to use the low-field magneto-transport as a tool to analyze the influence of a negative gate voltage. Figure 3(a) shows Hall data from one of the samples with large density tunability. It is a 10-nm-thick undoped  $\text{Bi}_2\text{Se}_3$  film. The electron density at  $V_G = 0$ , estimated from the low-field Hall resistance, is about  $2.7 \times 10^{13} \text{ cm}^{-2}$ . The Hall resistance,  $R_{xy}(B)$ , increases as  $V_G$  decreases. It reaches

a maximum at  $V_G = -125$  V, which would correspond to an electron density of  $n_e \approx 0.3 \times 10^{13} \text{ cm}^{-2}$ . Further decrease in  $V_G$  leads to smaller  $R_{xy}(B)$  and even reversal of its sign. For  $V_G < -150$  V, the Hall curves become strongly nonlinear. The high-field Hall coefficient is plotted in Fig. 3(b) and depends nonmonotonously on gate voltage.<sup>33</sup> The longitudinal resistivity at  $B = 0$ ,  $\rho_{xx}(0)$ , also exhibits a nonmonotonic dependence on  $V_G$ . This, together with the fact that the Hall coefficient  $R_H$  does not reach a minimum, points to the coexistence of electrons and holes for large negative gate voltages. It is noteworthy that the maximum in  $\rho_{xx}(0)$  appears at a  $V_G$  more negative than that of the  $R_H$  maximum. Therefore, the crossover from the pure electron system to the electron-hole system probably takes place before the appearance of the  $\rho_{xx}(0)$  maximum as  $V_G$  decreases.

For the gate voltages more negative than that at the  $R_{xy}$  maximum, the Fermi energies on the bottom and top surfaces are expected to lie below and above the Dirac point, respectively, even though the precise position of  $E_F$  is not known. As a consequence, the Fermi energy in the bulk (or at least part of the bulk) must be located in the band gap. The nearly one order of magnitude increase in  $\rho_{xx}(0)$  as  $V_G$  is lowered from 0 to  $-150$  V is much larger than what has been reported for cleaved  $\text{Bi}_2\text{Se}_3$  flakes cleaved on  $\text{SiO}_2/\text{Si}$  substrates.<sup>8</sup> The significantly enhanced  $\rho_{xx}(0)$  is an encouraging signature that much of the bulk conductivity can be suppressed. It can reach values as high as  $\sim h/e^2$ .<sup>7</sup>

The magnetoconductivity also exhibits a strong gate-voltage dependence, especially for  $V_G < -50$  V. Best fits to Eq. (1) yield the data plotted in Fig. 3(c). The most striking feature is that  $\alpha$  is close to  $1/2$  for  $V_G > -70$  V, and it increases to values close to 1 for  $V_G < -140$  V. In the crossover region ( $-70$  to  $-140$  V), the  $\text{Bi}_2\text{Se}_3$  thin film undergoes a transition from a low-density electron system to a separated electron-hole system. Hence, for large negative gate voltages with decoupled top and bottom layers, a fit of the  $\Delta\sigma_{xx}(B)$  data to a two-component HLN equation is more appropriate:

$$\Delta\sigma(B) \simeq -\frac{e^2}{2\pi h} \sum_{i=1}^2 \left[ \psi \left( \frac{1}{2} + \frac{B_{\phi i}}{B} \right) - \ln \left( \frac{B_{\phi i}}{B} \right) \right]. \quad (2)$$

Here,  $B_{\phi 1}$  and  $B_{\phi 2}$  are dephasing fields for conducting components 1 and 2, respectively. As shown in Fig. 3(d), they have opposite dependencies on  $V_G$ .  $B_{\phi 1}$  ( $B_{\phi 2}$ ) decreases (increases) as  $V_G$  is lowered. They approach approximately the same value for large negative gate voltages. The dephasing field is proportional to  $(D\tau_\phi)^{-1}$  with  $D \propto v_F^2 \tau_e$ , and  $\tau_\phi^{-1}$  increases with decreasing  $D$  because the main dephasing mechanism at low  $T$  is the  $e$ - $e$  interactions.<sup>30</sup> Consequently,  $B_\phi$  is expected to increase for the electron component on the top surface, while it should decrease for the holes at the bottom surface (interface) with decreasing  $V_G$ . Therefore, the two curves with larger and smaller values of  $B_\phi$  in Fig. 3(d) could be assigned to the bottom and top surfaces, respectively.

The observation that  $\alpha$  increases toward 1 based on fits of the magnetoconductivity data to the single-component HLN equation [Eq. (1)] implies that the top and bottom surfaces of the film make separate contributions to the conductivity.<sup>8,34</sup> Obtaining  $\alpha$  values close to 1, however, not only requires two

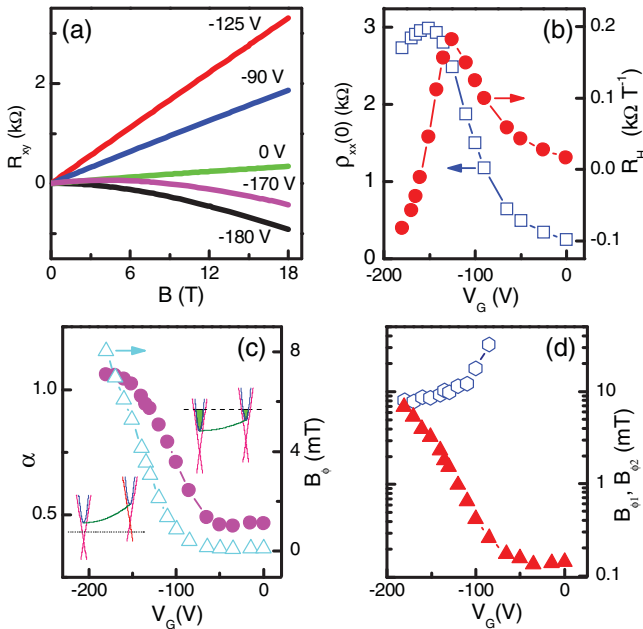


FIG. 3. (Color online) (a) Hall resistance curves for  $V_G = -125$ ,  $-90$ ,  $0$ ,  $-170$ , and  $-180$  V (from top to bottom). (b) Gate-voltage dependence of  $\rho_{xx}$  at  $B = 0$  and high-field Hall coefficient, defined as  $dR_{xy}/dB$  and fitted from the data in  $B = 16$ – $18$  T. (c)  $V_G$  dependence of  $\alpha$  and  $B_\phi$  obtained from fits to Eq. (1). The left and right insets show the schematic sketches of the band diagrams for large and small negative gate voltages, respectively. The top (bottom) surface is depicted on the left (right). (d)  $V_G$  dependence of  $B_{\phi 1}$  (hexagons) and  $B_{\phi 2}$  (triangles) obtained from fits to Eq. (2).  $B_{\phi 1}$  and  $B_{\phi 2}$  can be assigned to the bottom and top surfaces, respectively. This 10-nm-thick sample only has a back gate.

decoupled conduction channels, but also demands that both conduction channels have nearly identical dephasing fields. In general, this is hard to achieve, in particular, for samples where the gate tunability is not sufficient or the substrate surface is too rough.<sup>7</sup> Caution should also be taken to ensure that the transport is in the diffusive and weakly disordered ( $k_{Fl} \gg 1$ ) regime for which the HLN equation is valid. For highly resistive samples, e.g.,  $\rho_{xx} \sim h/e^2$  as shown in Ref. 7, the condition  $k_{Fl} \gg 1$  is no longer satisfied.

In conclusion, it is possible to identify the surface transport of 3D topological insulators from magnetoconductivity measurements when transport takes place in the weakly disordered, diffusive regime. The use of a high- $k$  dielectric such as SrTiO<sub>3</sub> for back gating enables us to tune the transport properties of both the top and the bottom surfaces. This

device geometry is particularly useful for the future exploration of hybrid devices in which a TI is interfaced with other materials.<sup>15–17</sup> The capability in creating comparable electron and hole conductivities on the opposite surfaces of TI thin films may also offer opportunities for unveiling novel quantum phenomena.<sup>18</sup>

We are grateful to L. Fu, D. Goldhaber-Gordon, I. V. Gornyi, A. D. Mirlin, P. M. Ostrovsky, V. Sacksteder, K. von Klitzing, X. C. Xie, and P. Xiong for valuable discussions. This work was supported by MOST-China (Grants No. 2007CB936800 and No. 2009CB929101) and NSF-China (Grants No. 10874210 and 10974240), and Chinese Academy of Sciences and German Ministry of Science and Education.

- <sup>1</sup>X. L. Qi and S.-C. Zhang, *Phys. Today* **63**, 33 (2010); M. Z. Hasan and C. L. Kane, *Rev. Mod. Phys.* **82**, 3045 (2010); M. Z. Hasan and J. E. Moore, *Ann. Rev. Cond. Matt. Phys.* **2**, 55 (2011).
- <sup>2</sup>D. Hsieh *et al.*, *Nature (London)* **452**, 970 (2008); L. Fu and C. L. Kane, *Phys. Rev. B* **76**, 045302 (2007).
- <sup>3</sup>D. Hsieh *et al.*, *Science* **323**, 919 (2009); Y. Xia *et al.*, *Nat. Phys.* **5**, 398 (2009); H. J. Zhang *et al.*, *ibid.* **5**, 438 (2009).
- <sup>4</sup>L. Fu and C. L. Kane, *Phys. Rev. Lett.* **100**, 096407 (2008); X. L. Qi *et al.*, *Science* **323**, 1184 (2009).
- <sup>5</sup>P. M. Ostrovsky, I. V. Gornyi, and A. D. Mirlin, *Phys. Rev. Lett.* **105**, 036803 (2010).
- <sup>6</sup>P. Roushan *et al.*, *Nature (London)* **460**, 1106 (2009); T. Zhang *et al.*, *Phys. Rev. Lett.* **103**, 266803 (2009).
- <sup>7</sup>J. Chen *et al.*, *Phys. Rev. Lett.* **105**, 176602 (2010).
- <sup>8</sup>J. G. Checkelsky, Y. S. Hor, R. J. Cava, and N. P. Ong, *Phys. Rev. Lett.* **106**, 196801 (2011).
- <sup>9</sup>H. T. He, G. Wang, T. Zhang, I. K. Sou, G. K. L. Wong, J. N. Wang, H. Z. Lu, S. Q. Shen, and F. C. Zhang, *Phys. Rev. Lett.* **106**, 166805 (2011).
- <sup>10</sup>M. Liu *et al.*, *Phys. Rev. B* **83**, 165440 (2011).
- <sup>11</sup>J. Wang *et al.*, e-print arXiv:1012.0271 (2010).
- <sup>12</sup>D. Hsieh *et al.*, *Nature (London)* **460**, 1101 (2009).
- <sup>13</sup>Y. L. Chen *et al.*, *Science* **325**, 178 (2009).
- <sup>14</sup>G. Bergmann, *Phys. Rep.* **107**, 1 (1984); S. Kobayashi and F. Komori, *Prog. Theor. Phys. Suppl.* **84**, 224 (1985).
- <sup>15</sup>L. Fu and C. L. Kane, *Phys. Rev. Lett.* **102**, 216403 (2009).
- <sup>16</sup>A. R. Akhmerov, J. Nilsson, and C. W. J. Beenakker, *Phys. Rev. Lett.* **102**, 216404 (2009).
- <sup>17</sup>I. Garate and M. Franz, *Phys. Rev. Lett.* **104**, 146802 (2010).
- <sup>18</sup>B. Seradjeh, J. E. Moore, and M. Franz, *Phys. Rev. Lett.* **103**, 066402 (2009); R. Yu *et al.*, *Science* **329**, 61 (2010); J. J. Zhu, D. X. Yao, S. C. Zhang, and K. Chang, *Phys. Rev. Lett.* **106**, 097201 (2011).
- <sup>19</sup>S. Hikami, A. I. Larkin, and Y. Nagaoka, *Prog. Theor. Phys.* **63**, 707 (1980).
- <sup>20</sup>A. A. Taskin and Y. Ando, *Phys. Rev. B* **80**, 085303 (2009); D. X. Qu *et al.*, *Science* **329**, 821 (2010); J. G. Analytis *et al.*, *Nat. Phys.* **6**, 960 (2010); Z. Ren, A. A. Taskin, S. Sasaki, K. Segawa, and Y. Ando, *Phys. Rev. B* **82**, 241306 (2010).
- <sup>21</sup>H. Peng *et al.*, *Nature Mater.* **9**, 225 (2010); F. X. Xiu *et al.*, *Nature Nanotech.* **6**, 216 (2011); Y. Y. Qin *et al.*, e-print arXiv:1012.0104.
- <sup>22</sup>G. H. Zhang *et al.*, *Adv. Funct. Mater.*, doi:10.1002/adfm.201002667.
- <sup>23</sup> $\alpha \simeq 1/2$  was also obtained previously from Bi<sub>2</sub>Se<sub>3</sub> thin films on Si by F. Yang *et al.* (unpublished).
- <sup>24</sup>Y. Kawaguchi and S. Kawaji, *Surf. Sci.* **113**, 505 (1982).
- <sup>25</sup>H. Fukuyama, in *Electron-Electron Interactions in Disordered Systems*, edited by A. L. Efros and M. Pollak (North-Holland, Amsterdam, 1985).
- <sup>26</sup>S. Maekawa and H. Fukuyama, *J. Phys. Soc. Jpn.* **50**, 2516 (1981).
- <sup>27</sup>P. A. Lee and T. V. Ramakrishnan, *Rev. Mod. Phys.* **57**, 287 (1985).
- <sup>28</sup>B. L. Altshuler, A. G. Aronov, and A. Y. Zuzin, *Solid State Commun.* **44**, 137 (1982).
- <sup>29</sup>H. Koehler and E. Wuchner, *Phys. Status Solidi B* **67**, 665 (1975).
- <sup>30</sup>B. L. Altshuler and A. G. Aronov, in *Electron-Electron Interactions in Disordered Systems*, edited by A. L. Efros and M. Pollak (North-Holland, Amsterdam, 1985).
- <sup>31</sup>A. Sahnoune, J. O. Strom-Olsen, and H. E. Fischer, *Phys. Rev. B* **46**, 10035 (1992).
- <sup>32</sup>A. D. Mirlin (private communications).
- <sup>33</sup>In the semiclassical model, more mobile carriers have more contributions in the low field  $R_{xy}$ . In contrast, the total carrier density determines  $R_{xy}$  in the high- $B$  limit.
- <sup>34</sup>H. Steinberg *et al.*, e-print arXiv:1104.1404; D. Kim *et al.*, e-print arXiv:1105.1410.